Journal of Medicinal Chemistry

Brief Article

Optimization of Chromeno[2,3-c]pyrrol-9(2H)-ones as Highly Potent, Selective, and Orally Bioavailable PDE5 Inhibitors: Structure-Activity Relationship, X-ray Crystal Structure, and Pharmacodynamic Effect on Pulmonary Arterial Hypertension

Deyan Wu, Yadan Huang, Yiping Chen, Yi-you Huang, Haiju Geng, Tianhua Zhang, Chen Zhang, Zhe Li, Lei Guo, Jianwen Chen, and Hai-Bin Luo

J. Med. Chem., **Just Accepted Manuscript** • DOI: 10.1021/acs.jmedchem.8b01209 • Publication Date (Web): 27 Aug 2018

ACS Publications

is published by the American Chemical Society. 1155 Sixteenth Street N.W., Washington, DC 20036

Optimization of Chromeno[2,3-c]pyrrol-9(2H)-ones as Highly Potent, Selective, and Orally Bioavailable PDE5 Inhibitors: Structure-Activity Relationship, X-ray Crystal Structure, and Pharmacodynamic Effect on Pulmonary Arterial Hypertension

Deyan Wu‡, Yadan Huang‡, Yiping Chen‡, Yi-You Huang, Haiju Geng, Tianhua Zhang, Chen Zhang, Zhe Li, Lei Guo, Jianwen Chen, Hai-Bin Luo*

School of Pharmaceutical Sciences, Sun Yat-Sen University, Guangzhou 510006, P. R. China.

ABSTRACT: To further explore the structure-activity relationship around the chromeno[2,3-c]pyrrol-9(2H)-one scaffold, nineteen derivatives as inhibitors against PDE5 were discovered. The most potent inhibitor **3** has an IC_{50} of 0.32 nM with remarkable selectivity and druglike profile. Oral administration of **3** (1.25 mg/kg) caused comparable therapeutic effects to sildenafil (10.0 mg/kg) against pulmonary arterial hypertension. Further, different binding patterns from sildenafil were revealed in co-crystal structures, which provide structural templates for discovery of highly potent PDE5 inhibitors.

INTRODUCTION

Pulmonary arterial hypertension (PAH) is a severely progressive and debilitating chronic illness that induces high pressure in the pulmonary arteries, leading to right-heart failure and eventual death.[1,2] Recently, significant advances in PAH pathology have been achieved for the development of several effective therapeutic targets in this disease and three signal pathways have been validated for its pathogenesis and progression (endothelin pathway, prostacyclin pathway, and NO/cGMP pathway).[3-5] In general, the inhibition of phosphodiesterase-5 (PDE5) via the NO/cGMP signal pathway[6,7], would lead to pulmonary vasodilation and smooth muscle cell growth inhibition[5,8]. Currently, two famous PDE5 inhibitors such as sildenafil and tadalafil were clinically used as anti-PAH agents.[3,5,9,10] Compared with other anti-PAH drugs, PDE5 inhibitors have relatively few adverse effects and are safe for patients who are with mild to moderate renal or hepatic dysfunction.[11,12]

Recently, we reported several chromeno[2,3-c]pyrrol-9(2H)-one analogues as potent inhibitors against PDE5.[13,14] Among them, compound **1** (Figure 1) exhibits an inhibitory affinity (IC50) of 5.6 nM and could be used as a lead against PAH. To further explore the structure-activity relationships around the scaffold and enrich their molecular diversity, compound **2** was identified as a potent intermediate inhibitor towards PDE5. Subsequently, the co-crystal structure of PDE5 with bound **11b** showed **11b** occupies the active pocket with a different binding mode from sildenafil. Based on the binding mode of the PDE5-**11b** complex, we further designed and synthesized five compounds as potent inhibitors. As a result, compound **3** exhibits a highly potent affinity of 0.32 nM with remarkable pharmacodynamic effects and druglike profile (metabolic stability, inhibition of hERG potassium channels, cytochrome P450 inhibition, plasma protein binding, and pharmacological safety), indicating that **3** could be used as a promising treatment or chemical probe against PAH.

RESULTS AND DISCUSSION

Chemistry. As shown in Scheme 1-3, we developed an efficient route to obtain derivatives **2-3**, **11a-m**, **16**, and **17a-c**. Herein, we use compound **4** as the starting material (Scheme 1), and it was treated with diodomethane and K2CO3 in acetonitril to acquire the intermediate **5**, followed by treatment with NaOH to afford the acid **6**.[15,16] The Boc group of compound **6** was deprotected by TFA in dichloromethane to generate the amino acid **7**.[17] Then, the Fmoc group was introduced with FmocCl and aqueous Na_2CO_3 in dioxane to yield the N-Fmoc amino acid (**8**).[14,18] Compounds **10a-10n** were synthesized by the reaction of ethyl thiazole-2-carboxylate (**9**) and 2'-hydroxyacetophenones in toluene with the base of sodium hydride. Then, compounds **2** and **11a-m** were synthesized as previously reported steps.[13,14,19] Compounds **3**, **16**, and **17a-c** were synthesized through the route outlined in Scheme 3. Additionally, 3-Fluoro-5-bromophenol (**12**) was acetylated with acetyl chloride and followed by Friedel-Crafts acetylation to afford 1-(4-bromo-2-fluoro-6-hydroxyphenyl)ethenone (**14**).[20]

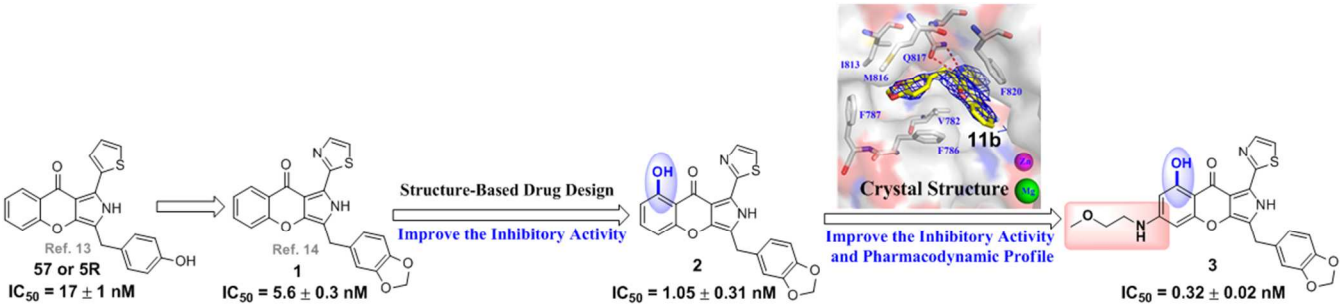

Figure 1. Structural optimization of compound **1** resulted in novel and highly potent PDE5 inhibitors with improved pharmacodynamic profile.

Then, the same procedures as Scheme 2 were used to yield compound **16**, which was coupled with amines to afford **3,** and **17a-c** via Buchwald-Hartwig cross coupling reaction, respectively. Experimental and analytical information for **2-3**, **11a-m**, **16**, and **17a-c** are provided in the Supporting Information.

PAINS screening of the newly designed nineteen derivatives was carried out via an online program "PAINS Remover" (http://www.cbligand.org /PAINS)[21] in order to prevent false positive results, and all the derivatives passed this screening.

Structure–Activity Relationships (SARs).

We previously reported several chromeno[2,3-c]pyrrol-9(2H)-one inhibitors towards PDE5 as anti-PAH agents, and lead **1** has an IC50 of 5.6 nM.[13,14] Herein, to further explore and enrich the structure-activity relationships around the scaffold, nineteen derivatives were synthesized. Their inhibitory activities against PDE5 are showed in Table 1 and all the derivatives show considerable inhibitory potencies (less than 10 nM). Specifically, compounds **2** and **11a-11b** have a different substitution at the 6-position, in which the introduction of OH/F groups (**2** and **11b**, IC_{50} = 1.05 nM and 1.41 nM, respectively) at the 6-position resulted in tighter binding than that with methoxyl group (**11a**). Comparing compounds **11b**, **11d**, and **11j** with fluorine substitutions at the 6-position, 5-position, and 4-position, respectively, **11b** shows the best IC_{50} of 1.41 nM, which indicates that fluorine atoms in the 6-position possibly favor the binding mode of chemicals with PDE5. Comparing compounds **11m**, **11e**, and **11k** with chlorine substitutions at the 3-position, 4-position, and 5-position, respectively, **11e** shows the worst IC_{50} of 9.63 nM, which indicates that halogen atoms in the 5-position possibly disfavor the binding mode of chemicals with PDE5. A similar trend is observed for **11f** and **11l** or **11d** and **11j**. Thus, compounds**2** and **11b** were identified as potent intermediate inhibitors for subsequent study.

Scheme 1. Synthesis of (S)-2-(Fmoc-amino)-3-(benzo[d][1,3]dioxol-5-yl)propanoic acid. [a]

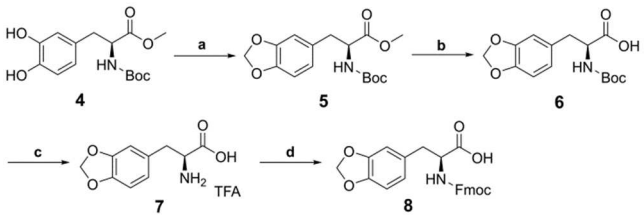

[a]Reagents and conditions: (a) diodomethane, K_2CO_3, acetonitril, ref. 16h; (b) 1N NaOH, MeOH, rt, 4 h; (c) TFA, DCM, rt, 1 h; (d) 9-Fluorenylmethyl chloroformate, dioxane, H_2O, 0°C, 1 h, rt, 1 h.

Scheme 2. Synthesis of compounds **2** and **11a-m**. [a]

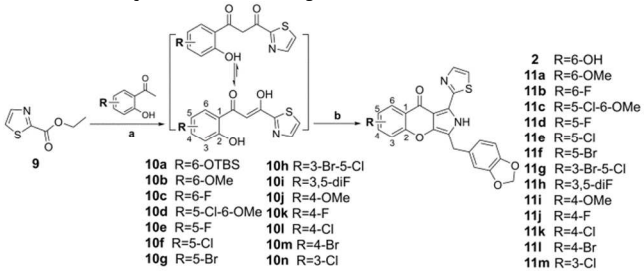

[a]Reagents and conditions: (a) NaH, toluene, 0°C to 60°C, 2 h; (b) **8**, DMAP, DCC, pyridine, rt, 3 h, 50°C, 6 h.

Scheme 3. Synthesis of compounds **3** and **17a-c**. [a]

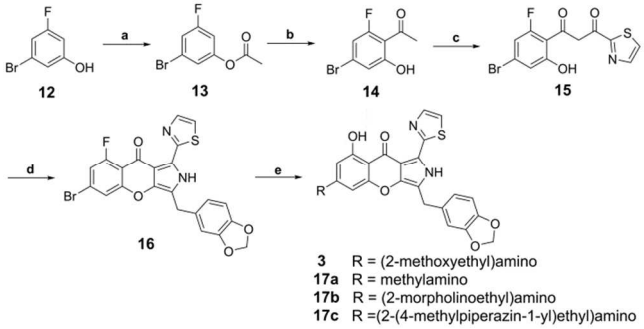

[a]Reagents and conditions: (a) Ac_2O, NaOAc, 110°C, 2 h; (b) $AlCl_3$, 140°C, 3 h; (c) **9**, NaH, toluene, 0°C to 60°C, 2 h; (d) **8**, DMAP, DCC, pyridine, rt, 3 h, 50°C, 6 h; (e) RNH_2, $Pd(dppf)_2Cl_2$, BINAP, t-BuONa, DMSO, 100°C, 24 h.

Table 1. Structure–Activity Relationships of Compounds 2 and 11a-m[a]

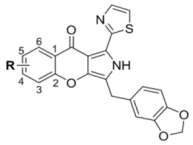

Compound	R	IC_{50} (nM)
2	6-OH	1.05±0.31
11a	6-OMe	4.38±0.32
11b	6-F	1.41±0.30
11c	5-Cl-6-OMe	6.82±0.34
11d	5-F	4.03±0.14
11e	5-Cl	9.63±1.09
11f	5-Br	3.82±0.10
11g	3-Br-5-Cl	3.04±0.22
11h	3,5-diF	1.63±0.24
11i	4-OMe	2.64±0.39
11j	4-F	2.38±0.31
11k	4-Cl	2.64±0.27
11l	4-Br	1.58±0.23
11m	3-Cl	2.09±0.15

[a]Sildenafil, the reference compound (IC_{50}=5.1 nM).

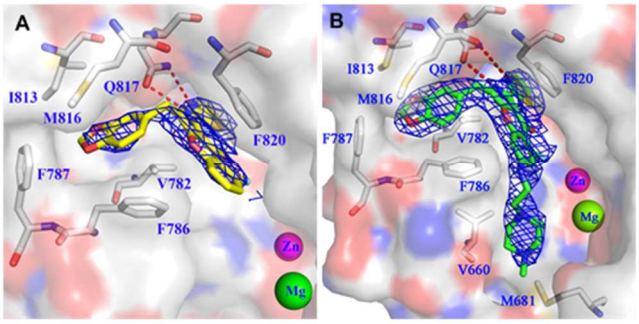

Figure 2. Co-crystal structures of the PDE5-**11b** and PDE5-**17c** complexes (PDB ID: 5ZZ2 and 6ACB). (A) Surface model of **11b** with PDE5 (yellow sticks); (B) Surface model of **17c** with PDE5 (green sticks). The dotted lines refer to H-bonds.

Crystal structure of PDE5 with bound 11b. To determine where compound **11b** bind, the unliganded PDE5 and its complex were crystallized by the hanging drop method. In Figure 2A, **11b** captured the same pocket as typical PDE5 inhibitors, except with a different binding model. The main skeleton of **11b** is clamped by three hydrophobic residues Val782, Phe786, and Phe820. In addition, the pyrrol ring (NH) of **11b** involves an H-bond of 2.8 Å with the amide oxygen of residue Gln817, and the thiazole ring (S or N) of **11b** also makes an H-bond with the amide nitrogen of residue Gln817 (3.3 Å to the nitrogen) along with hydrophobic interactions with other residues (such as Ala767, Ile768, Gln775, and Ile778). The electron density maps of (2Fo-Fc) and (Fo-Fc) clearly revealed the binding mode of PDE5 with **11b**, in which the thiazole ring conjugated with the purine ring. Compared with our previously reported inhibitor **5R**[13] (Figure 1), **11b** interacts much tightly with four hydrophobic residues Val782, Phe787, Ile813, and Met816. Notably, the benzene ring of **11b** is outside the binding pattern, which explains why most of the compounds listed in Table 1 have improved inhibitory activities towards PDE5, and different substituents on this ring can be further optimized.

Based on the acquired binding pattern of **11b**, we further synthesized another series as potent PDE5 inhibitors based on the 4-position of the benzene ring outside the binding pattern (Table 2). The results indicated that all the compounds showed improved inhibitory activities except **16**, which has a bromine atom at the 4-position and a fluorine atom at the 6-position. It is gratifying to see that compound **3**, with a (2-methoxyethyl)amino substitution at the 4-position, exhibits the most potent inhibition of IC_{50} = 0.32 nM. Finally, compound **3** was selected as the candidate for subsequent study.

Crystal structure of PDE5 with bound 17c. Given the promising biological activities of compounds **17a-c** and **3**, we tried to acquire their crystal structures with PDE5. Among them, the co-crystal structure of PDE5 with **17c** was finally obtained (Figure 2B). The structure indicated that **17c** have the same binding pattern as **11b**, but **17c** have another substitution at the 4-position and forms hydrophobic interactions with the residues Val660 and Met681. As a result, compounds **3** and **17a-c** resulted in tighter binding than compound **2**, and exhibit highly potent PDE5 inhibition.

Table 2. Structure–Activity Relationships of Compounds 3, 16, and 17a-c.

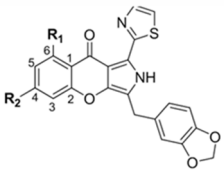

Compound	R1	R2	IC_{50} (nM)
2	OH	H	1.05±0.31
16	F	Br	2.37±0.17
17a	OH	CH_3	0.52±0.09
17b	OH	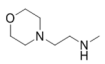	0.79±0.03
18	OH	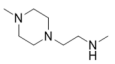	0.39±0.05
3	OH	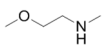	0.32±0.02

High selectivity of compound 3 against other PDE families. We have measured the selectivity index of compound **3** against other PDE subtypes (Table 3). Compound **3** exhibited at least 1000-fold selectivity over PDE1B, PDE3A, PDE7A1, PDE8A1, and PDE9A2. Additionally, the selectivity index values against PDE2A, PDE10A, PDE4D2, and PDE6C were 331-fold, 144-fold, 134-fold, and 4-fold higher than those against PDE5A1, respectively. Under identical assay condition, the reference drug sildenafil or vardenafil had a similar selectivity index of 5-fold or 3-fold to **3** against PDE6C. Specially, **3** exhibited a higher selectivity of 122-fold against PDE11A than the reference drug tadalafil of 20-fold. In short, compound **3** gives high selectivity over other PDEs except PDE6C.

Table 3. Selectivity index of 3 across PDE Families.

PDE isozyme	**3**	
	IC50 (nM)	Selectivity index
PDE5A1(535-860)	0.32 ± 0.02	-
PDE1B(10-487)	>32 000	>10 000
PDE2A(580-919)	106 ±3	331
PDE3A(679-1087)	>32 000	>10000
PDE4D2(86-413)	43 ± 1	134
PDE6C(1-858)	1.2 ± 0.1	4[a]
PDE7A1(130-482)	>32 000	>10 000
PDE8A1(480-820)	>32 000	>10 000
PDE9A2(181-506)	>32 000	>10 000
PDE10A(449-770)	46 ± 3	144
PDE11A(588-911)	39.0±0.4	122[b]

[a]Under identical assay condition, the reference drug sildenafil or vardenafil had a similar selectivity index of 5-fold or 3-fold to **3** against PDE6C; [b]Under identical assay condition, the reference drug tadalafil had a selectivity index of 20-fold against PDE11A.

Reasonable druglike profile. Since compound **3** exhibited subnanomolar inhibition against PDE5 and excellent selectivity over other PDEs, its druglike profile evaluations were performed. Table 4 shows that compound **3** was stable in rat liver microsomes with $T_{1/2}$ of 15.07 min and E_h of 75%, respectively, which is significantly better than the other compounds of **11b**(9.52 min and 83%), **17c** (5.26 min and 90%), and reference drug sildenafil (5.37 min and 89%). Other druglike profile evaluations are shown in Table 5, such as cytochrome P450 inhibition (**3** has an IC_{50} of > 10 μM against CYP1A2, 2B6, 2D6, and 3A4 and 0.135 μM against CYP2C9, respectively), inhibition of hERG potassium channels (IC_{50}> 30 μM), plasma protein binding (PPB) (97.74%), and pharmacological safety (**3** was well tolerated up to a dose of 1.5 g/kg and with no acute toxicity). These results indicate that compound **3** could be used as a promising candidate for further development.

Notable therapeutic effects against PAH in rats. The therapeutic results of compound **3** as anti-PAH agents *in vivo* are shown in Figure 3. A dramatical reduction of mean pulmonary artery pressure (mPAP) for the control group was observed compared with that of the model group, while the index of right ventricle hypertrophy (RVHI) of the control group was significantly decreased than that of the model group, which demonstrated the rats was successfully induced with PAH after 3 weeks monocrotaline (MCT) injection. As a result, the average mPAPs (19.94 mmHg and 20.86 mmHg) of the groups treated with **3** and sildenafil citrate at oral doses of 1.25 mg/kg and 10.0 mg/kg were significantly decreased compared with the model group (52.55 mmHg, Figure 3A). For the RVHI values, similar phenomena were also observed. It was clear that compound **3** at dose 1.25 mg/kg caused better therapeutic effects on both mPAP and RVHI than sildenafil citrate at dose 10.0 mg/kg (Figure 3B). Additionally, the wall thickness percentage (WT %) of the external diameter for the model group was significantly increased as well. As shown in Figure 3C, compound **3** and sildenafil citrate showed remarkable reduction to the WT% values compared with the model group and performed well.

Table 4. Metabolic Stability of Compounds 11b, 17c, and 3 in Rat Liver Microsomes.

Compound	k	$T_{1/2}$ (min)	Cl_{int} (mL/min/mg)	Cl_{app} (mL/min/kg)	Cl_h (mL/min/kg)	E_h (%)
11b[a]	0.0728	9.52	0.1456	262.13	45.46	83%
17c[b]	0.1317	5.26	0.2634	472.01	49.42	90%
3[a]	0.0378	18.33	0.0756	136.09	39.17	71%
3[b]	0.0460	15.07	0.0920	164.86	41.35	75%
sildenafil[b]	0.1291	5.37	0.2582	462.69	49.32	89%

[a] the first experiment; [b] the second experiment.

Table 5. The DruglikeProfile of Compound 3.

Rat liver microsomes ($T_{1/2}$)	hERG inhibition (IC_{50})	CYP P450 inhibition (IC_{50})	Plasma protein binding	Acute safety
15.07 min	>30 μM	> 10 μM（CYP1A2, 2B6, 2D6, and 3A4) 135 nM(CYP2C9)	97.7%	> 1.5 g/kg

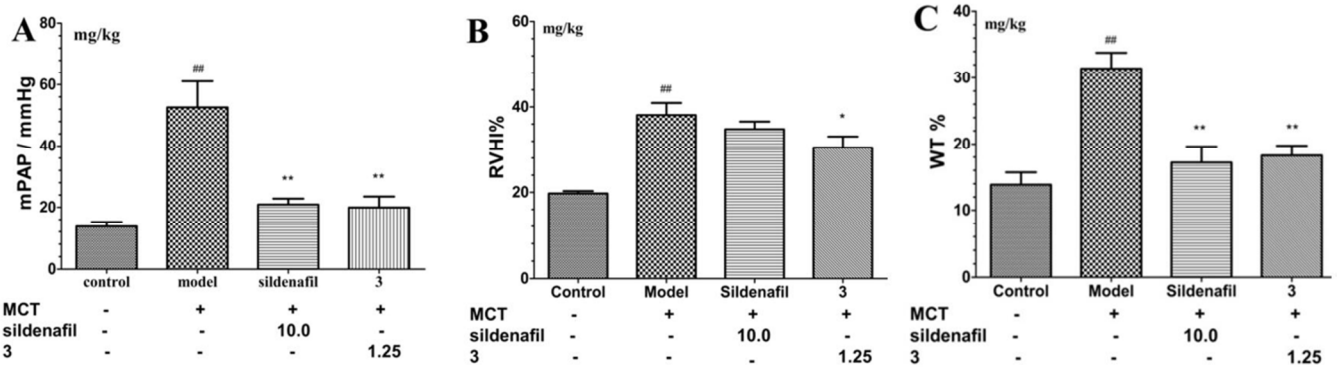

Figure 3. Significant effects of compound **3** and sildenafil citrate on pulmonary arterial remodeling of rats *in vivo*. (A) Dramatical reduction of hypertension pressure by **3** and sildenafil citrate, which was firstly induced by monocrotaline (MCT). Comparison of the mPAP values between different groups was provided in (A). (B) Effects of **3** and sildenafil citrate on RVHI of PAH model rats. Comparison of the RVHI% values between different groups was provided in (B). (C) Effects of **3** and sildenafil citrate on the wall thickness percentage (WT%) of small pulmonary arteries of PAH model rats. Comparison of the WT % values between different groups was provided in (C). Here, the data is shown as the mean ± S.E.M (n = 6-9 per group), and (##) refers to $p < 0.01$ compared to the control group; (∗) refers to $p < 0.05$ compared to the model group ,(∗∗) refers to $p < 0.01$ compared to the model group.

CONCLUSION

In summary, nineteen newly designed derivatives as PDE5 inhibitors were discovered with IC_{50} uniformly < 10 nM. Medicinal optimization resulted in the most potent inhibitor **3** with IC_{50} of 0.32 nM against PDE5 with high selectivity against other PDE subtypes. After druglike properties evaluations, oral administration of **3** at dose 1.25 mg/kg caused comparable therapeutic effects to sildenafil citrate at dose 10.0 mg/kg against PAH. The co-crystal structure of PDE5 with bound **17c** reveals a different binding pattern from sildenafil. In short, this work provides not only a molecular basis for understanding their recongnition mechanism, but also the structural templates for discovery of highly potent PDE5 inhibitors.

EXPERIMENTAL SECTION

General Methods. All starting materials and reagents were purchased from commercial suppliers (Adamas, Bide, Energy, Meryer, Sigma-Aldrich, and J&K) and used directly without further purification. Silica gel plates with fluorescence F254 (0.1-0.2 mm, Huanghai®) were used for thin-layer chromatography (TLC) analysis, and chemical HG/T2354-92 silica gel (200-300 mesh, Haiyang®) was used for column chromatography. Reactions requiring anhydrous conditions were performed under argon or a calcium chloride tube. ^{1}H NMR/^{13}C NMR spectra were recorded on a Bruker AVANCE III 400 instrument with tetramethylsilane as an internal standard. The following abbreviations are used: s (singlet), br (broad signal), d (doublet), dd (doublet of doublets), dt (doublet of triplets), t (triplet), td (triplet of doublets), q (quartet), and m (multiplet), and coupling constants are reported in Hz. High resolution mass spectra (HRMS) were recorded on a MAT-95 spectrometer. The purity of tested compounds were determined by reverse-phase high performance liquid chromatography (HPLC) analysis confirming to be more than 95%. HPLC instrument: SHIMADZU LC-20AT (Detector: SPD-20A UV/VIS detector, UV detection at 254 nm; column: Hypersil BDS C18, 5.0 μm, 4.6 × 150 mm (Elite); Elution, MeOH in water (70%-90%, v/v); T = 25°C; and flow rate = 1.0 mL/min.

General Procedure for Synthesis of Compounds 3. To a solution of **16** (500 mg, 1.0 mmol), 2-methoxyethanamine (225 mg, 3.0 mmol), and 2,2'-bis(diphenylphosphino)-1,1'-bisnaphthyl (124 mg, 0.2 mmol,) in DMSO (15 mL) was added 1,1'-bis(diphenylphosphino)ferrocene-palladium(II) dichloride dichloromethane complex (82 mg, 0.1 mmol) and sodium tert-butoxide (192 mg, 2.0 mmol). The mixture was then heated to 100°C for 24 h under an argon atmosphere. After the solution had cooled to room temperature it was diluted with EtOAc (150 mL) and washed with brine (3 × 100 mL). The organic layer was dried over anhydrous Na_2SO_4 and concentrated to give a crude, which was purified by silica gel column chromatography (petroleum ether:EtOAc, 4:1) to obtain the product **3** (182 mg) as a yellow solid. Yield: 37%; purity: 99%; ^{1}HNMR (500 M,

Acetone – d_6) δ 13.25 (s, 1H), 7.82 (d, J = 3.1 Hz, 1H), 7.59 (d, J = 3.1 Hz, 1H), 6.89 (s, 1H), 6.83 (d, J = 8.0 Hz, 1H), 6.76 (d, J = 7.9 Hz, 1H), 6.17 (s, 1H), 6.01 (s, 1H), 5.94 (s, 2H), 4.18 (s, 2H), 3.60 (t, J = 5.3 Hz, 2H), 3.43 (dd, J = 10.2, 5.1 Hz, 2H), 3.35 (s, 3H); ^{13}C NMR (101 MHz, DMSO – d_6) δ 178.23, 163.32, 159.06, 157.56, 155.90, 147.73, 146.11, 141.75, 141.50, 133.35, 121.56, 121.20, 119.26, 116.83, 109.20, 108.70, 108.10, 101.26, 99.81, 93.76, 89.75, 70.80, 58.52, 42.49, 29.32; HRMS (ESI) m/z calcd $C_{25}H_{22}N_3O_6S^+$ $[M+H]^+$ 492.1224, found 492.1223.

Protein expression and purification. The recombinant pET-PDE5A1 plasmid (catalytic domain, 535-860) was subcloned and purified by protocols reported previously.[14,22,23] After being transferred into the *E. coli* strain BL21 (Codonplus, Stratagene) for overexpression and growing in TB medium at 37°C until OD_{600} = 3-4, 0.1 mM isopropyl-β-D-thiogalactopyranoside (DTT) was added to induce PDE5A1 protein expression. The induced cells were collected after growing at 12°C for an additional 40-48 h. The PDE5A1 protein was purified through a Ni-NTA column (QIAGEN), Q-column (GE Healthcare) and Superdex 100 column (GE Healthcare). A typical batch of cells yielded over 10 mg of the PDE5A1 protein from 2 L of TB cell culture with a purity greater than 95% as shown by SDS–PAGE. The catalytic domains of PDE1B (10–487), PDE2A (580–919), PDE3A (679–1087), PDE4D (86–413), PDE7A (130–482), PDE9A (181–506), PDE8A (480–820), PDE10A (449–770), and PDE11A (588-911) were purified with similar protocols as previously reported.[13,24-27] PDE6C was purchased from BPS Bioscience.

ASSOCIATED CONTENT

Supporting Information

The Supporting Information is available free of charge on the ACS Publications website.

General Procedures for Bioassays, Crystallization trials, Druglike Profile of Compound **3**, General Procedures for the Synthesis of Chromeno[2,3-c]pyrrol-9(2H)-ones, and ^{1}H NMR, ^{13}C NMR, High-resolution mass spectra (HRMS) data for tested compounds.

Molecular formula strings and some data (CSV).

Accession Codes

The atomic coordinates and structure factors have been deposited into the RCSB Protein Data Bank with accession number 5ZZ2 and 6ACB.

AUTHOR INFORMATION

Corresponding Author

*H.-B. L.: phone, +86-20-39943031; fax, +86-20-39943000; e-mail, luohb77@mail.sysu.edu.cn.

ORCID

Hai-Bin Luo: 0000-0002-2163-0509

Author Contributions

‡These authors contributed equally.

Notes

The authors declare no competing financial interest.

ABBREVIATIONS USED

BINAP, (+/-)-2,2'-bis(diphenylphosphino)-1,1'-binaphthyl; Boc, t-butoxycarbonyl; cGMP, cyclic guanosine monophosphate; Clapp, apparent clearane; Cl_h, hepatic clearane; Cl_{int}, intrinsic clearane; CYP, cytochrome P450s; DCC, Dicyclohexylcarbodiimide; DCM, dichloromethane; DIPEA, ethyldiisopropylamine; DMAP, 4-Dimethylaminopyridine; Eh, hepatic extraction ratio; Fmoc-Cl, fluorenylmethoxycarbonyl chloride; hERG, the human Ether-a-go-go-Related Gene; MCT, monocrotaline; mPAP, Mean Pulmonary Artery Pressure; PAH, Pulmonary arterial hypertension; PDE, phosphodiesterase; PDE5, phosphodiesterase 5; RVHI, Index of Right Ventricle Hypertrophy; SAR, structure-activity relationship; $T_{1/2}$, half time; TFA, trifluoroacetic acid; TMS, tetramethylsilane.

ACKNOWLEDGMENT

This work was supported by the Natural Science Foundation of China (81522041, 21572279, 81602955, 81703341, and 21702238), Science Foundation of Guangdong Province (2016A030310144), the Fundamental Research Funds for the Central Universities (Sun Yat-Sen University) (17ykpy03 and 17ykpy20), Medical Scientific Research Foundation of Guangdong Province (A2016104), and Guangdong Province Higher Vocational Colleges & Schools Pearl River Scholar Funded Scheme (2016). We cordially thank Prof. H. Ke from Department of Biochemistry and Biophysics at the University of North Carolina (Chapel Hill) for his help with molecular cloning, expression, purification, crystal structure, and bioassay of PDEs.

REFERENCES

1. Voelkel, N. F.; Quaife, R. A.; Leinwand, L. A.; Barst, R. J.; McGoon, M. D.; Meldrum, D. R.; Dupuis, J.; Long, C. S.; Rubin, L. J.; Smart, F. W.; Suzuki, Y. J.; Gladwin, M.; Denholm, E. M.; Gail, D. B. Right Ventricular Function and Failure: Report of a National Heart, Lung, and Blood Institute Working Group on Cellular and Molecular Mechanisms of Right Heart Failure. *Circulation* **2006,***114*, 1883−1891.

2. Thenappan, T.; Shah, S. J.; Rich, S.; Gomberg-Maitland, M. A USA-based Registry for Pulmonary Arterial Hypertension: 1982-2006. *Eur. Respir. J.* **2007,***30*, 1103−1110.

3. Badesch, D. B.; Abman, S. H.; Simonneau, G.; Rubin, L. J.; McLaughlin, V. V. Medical therapy for Pulmonary Arterial Hypertension: Updated ACCP Evidence-based Clinical Practice Guidelines. *Chest* **2007,***131*, 1917−1928.

4. Montani, D.; Chaumais, M. C.; Savale, L.; Natali, D.; Price, L. C.; Jais, X.; Humbert, M.; Simonneau, G.; Sitbon, O. Phosphodiesterase Type 5 Inhibitors in Pulmonary Arterial Hypertension. *Adv. Ther.* **2009,***26*, 813−825.

5. Raja, S. G.; Raja, S. M. Treating Pulmonary Arterial Hypertension: Current Treatments and Future Prospects. *Ther. Adv. Chronic Dis.* **2011,***2*, 359−370.

6. Giordano, D.; De Stefano, M. E.; Citro, G.; Modica, A.; Giorgi, M. Expression of cGMP-binding cGMP-specific Phosphodiesterase (PDE5) in Mouse Tissues and Cell Lines Using an Antibody Against the Enzyme Amino-terminal Domain. *Biochim. Biophys. Acta, Mol. Cell Res.* **2001,***1539*, 16−27.

7. Rawson, D. J.; Ballard, S.; Barber, C.; Barker, L.; Beaumont, K.; Bunnage, M.; Cole, S.; Corless, M.; Denton, S.; Ellis, D.; Floc'h, M.; Foster, L.; Gosset, J.; Holmwood, F.; Lane, C.; Leahy, D.; Mathias, J.; Maw, G.; Million, W.; Poinsard, C.; Price, J.; Russel, R.; Street, S.;

Watson, L. The Discovery of UK-369003, A Novel PDE5 Inhibitor with the Potential for Oral Bioavailability and Dose-proportional Pharmacokinetics. *Bioorg. Med. Chem.* **2012,***20*, 498−509.
8. Raja, S. G.; Danton, M. D.; MacArthur, K. J.; Pollock, J. C. Treatment of Pulmonary Arterial Hypertension with Sildenafil: From Pathophysiology to Clinical Evidence. *J. Cardiothorac. Vasc. Anesth.* **2006,***20*, 722−735.
9. Humpl, T.; Reyes, J. T.; Holtby, H.; Stephens, D.; Adatia, I. Beneficial Effect of Oral Sildenafil Therapy on Childhood Pulmonary Arterial Hypertension. *Circulation* **2005,***111*, 3274−3280.
10. Galie, N.; Brundage, B. H.; Ghofrani, H. A.; Oudiz, R. J.; Simonneau, G.; Safdar, Z.; Shapiro, S.; White, R. J.; Chan, M.; Beardsworth, A.; Frumkin, L.; Barst, R. J. Tadalafil Therapy for Pulmonary Arterial Hypertension. *Circulation* **2009,***119*, 2894−2903.
11. Archer, S. L.; Michelakis, E. D., Phosphodiesterase Type 5 Inhibitors for Pulmonary Arterial Hypertension.*N. Engl. J. Med.***2009,***36*, 1864−1871.
12. Yanagisawa, R.; Kataoka, M.; Taguchi, H.; Kawakami, T.; Tamura, Y.; Fukuda, K.; Yoshino, H.; Satoh, T. Impact of First-Line Sildenafil Monotreatment for Pulmonary Arterial Hypertension. *Circ. J.* **2012,***76*, 1245−1252.
13. Shang, N. N.; Shao, Y. X.; Cai, Y. H.; Guan, M.; Huang, M.; Cui, W.; He, L.; Yu, Y. J.; Huang, L.; Li, Z.; Bu, X. Z.; Ke, H.; Luo, H.-B. Discovery of 3-(4-Hydroxybenzyl)-1-(thiophen-2-yl)chromeno[2,3-c]pyrrol-9(2H)-one as a Phosphodiesterase-5 Inhibitor and Its Complex Crystal Structure. *Biochem. Pharmacol.* **2014,***89*, 86−98.
14. Wu, D.; Zhang, T.; Chen, Y.; Huang, Y.; Geng, H.; Yu, Y.; Zhang, C.; Lai, Z.; Wu, Y.; Guo, X.; Chen, J.; Luo, H.-B. Discovery and Optimization of Chromeno[2,3-c]pyrrol-9(2H)-ones as Novel Selective and Orally Bioavailable Phosphodiesterase 5 Inhibitors for the Treatment of Pulmonary Arterial Hypertension. *J. Med. Chem.* **2017,***60*, 6622−6637.
15. Chang, J.; Chen, R.; Guo, R.; Dong, C.; Zhao, K. Synthesis, Separation, and Theoretical Studies of Chiral Biphenyl Lignans (α - and β - DDB). *Helv. Chim. Acta* **2003,***86*, 2239−2246.
16. Tran Van, C.; Nennstiel, D.; Scherkenbeck, J. Macrocyclic Analogues of the Diuretic Insect Neuropeptide Helicokinin I Show Strong Receptor-binding. *Bioorg. Med. Chem.* **2015,***23*, 3278−3286.
17. Muller, J.; Feifel, S. C.; Schmiederer, T.; Zocher, R.; Sussmuth, R. D. In Vitro Synthesis of New Cyclodepsipeptides of the PF1022-type: Probing the Alpha-D-hydroxy Acid Tolerance of PF1022 Synthetase. *Chembiochem* **2009,***10*, 323−328.
18. Jørgensen, M. R.; Olsen, C. A.; Mellor, I. R.; Usherwood, P. N. R.; Witt, M.; Franzyk, H.; Jaroszewski, J. W. The Effects of Conformational Constraints and Steric Bulk in the Amino Acid Moiety of Philanthotoxins on AMPAR Antagonism. *J. Med. Chem.* **2005,***48*, 56−70.
19. Yu, Y.; Hu, Y.; Shao, W.; Huang, J.; Zuo, Y.; Huo, Y.; An, L.; Du, J.; Bu, X. Synthesis of Multi-Functionalized Chromeno[2,3-c]pyrrol-9(2H)-ones: Investigation and Application of Baker-Venkataraman Rearrangement Involved Reactions Catalyzed by 4-(Dimethylamino)pyridine. *Eur. J. Org. Chem.* **2011,***2011*, 4551−4563.
20. Kónya, K.; Langer, P.; Jordán, S.; Pajtás, D.; Patonay, T. Synthesis of 6,7-Dibromoflavone and Its Regioselective Diversification via Suzuki–Miyaura Reactions. *Synthesis* **2017,***49*, 1983−1992.
21. Baell, J. B.; Holloway, G. A. New Substructure Filters for Removal of Pan Assay Interference Compounds (PAINS) from Screening Libraries and for Their Exclusion in Bioassays. *J. Med. Chem.* **2010,***53*, 2719−2740.
22. Li, Z.; Cai, Y. H.; Cheng, Y. K.; Lu, X.; Shao, Y. X.; Li, X.; Liu, M.; Liu, P.; Luo, H.-B. Identification of Novel Phosphodiesterase-4D Inhibitors Prescreened by Molecular Dynamics-augmented Modeling and Validated by Bioassay. *J. Chem. Inf. Model.* **2013,***53*, 972−981.
23. Lin, T. T.; Huang, Y. Y.; Tang, G. H.; Cheng, Z. B.; Liu, X.; Luo, H. B.; Yin, S. Prenylated Coumarins: Natural Phosphodiesterase-4 Inhibitors from Toddalia Asiatica. *J. Nat. Prod.* **2014,***77*, 955−962.
24. Park, S. J.; Ahmad, F.; Philp, A.; Baar, K.; Williams, T.; Luo, H.; Ke, H.; Rehmann, H.; Taussig, R.; Brown, A. L.; Kim, M. K.; Beaven, M. A.; Burgin, A. B.; Manganiello, V.; Chung, J. H. Resveratrol Ameliorates Aging-related Metabolic Phenotypes by Inhibiting cAMP Phosphodiesterases. *Cell* **2012,***148*, 421−433.
25. Shao, Y. X.; Huang, M.; Cui, W.; Feng, L. J.; Wu, Y.; Cai, Y.; Li, Z.; Zhu, X.; Liu, P.; Wan, Y.; Ke, H.; Luo, H.-B. Discovery of a Phosphodiesterase 9A Inhibitor as a Potential Hypoglycemic Agent. *J. Med. Chem.* **2014,***57*, 10304−10313.
26. Wang, H.; Yan, Z.; Yang, S.; Cai, J.; Robinson, H.; Ke, H. Kinetic and Structural Studies of Phosphodiesterase-8A and Implication on the Inhibitor Selectivity. *Biochemistry* **2008,***47*, 12760−12768.
27. Wang, H.; Liu, Y.; Chen, Y.; Robinson, H.; Ke, H. Multiple Elements Jointly Determine Inhibitor Selectivity of Cyclic Nucleotide Phosphodiesterases 4 and 7. *J. Biol. Chem.* **2005,***280*, 30949−30955.

Table of Contents Graphic.

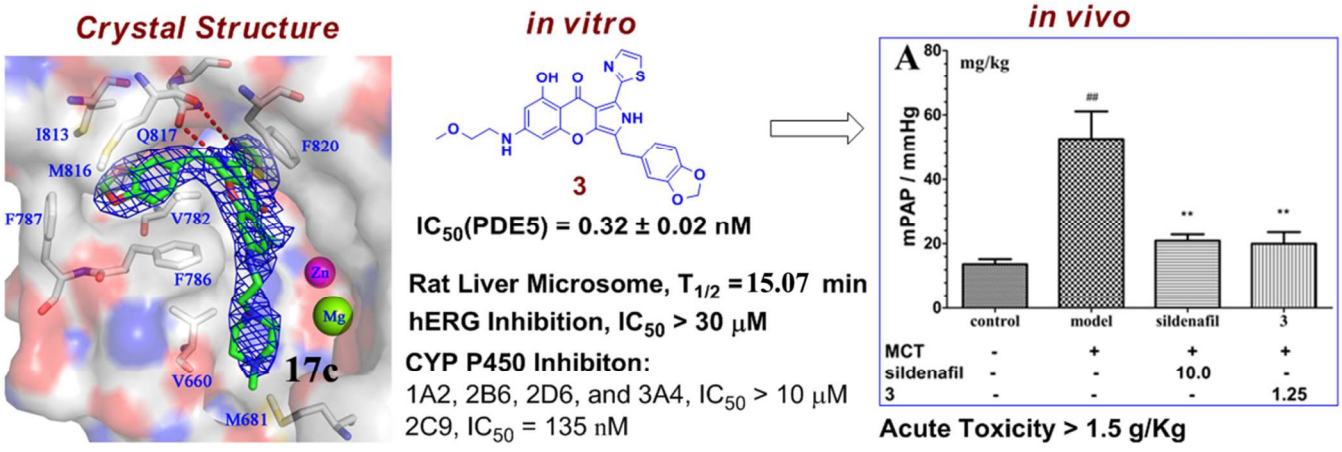

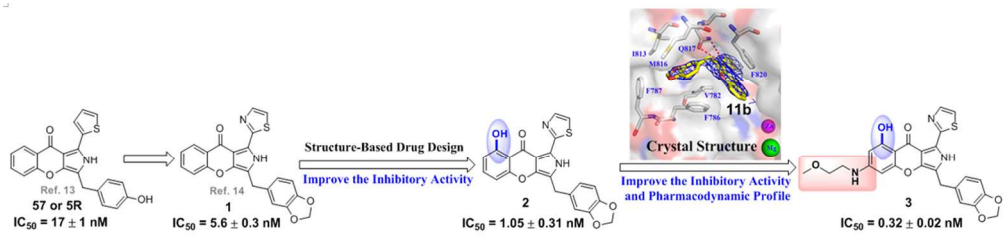

Figure 1. Optimization of chromeno[2,3-c]pyrrol-9(2H)-ones as novel PDE5 inhibitors with improved inhibitory activity and pharmacodynamic profile.

337x77mm (200 x 200 DPI)

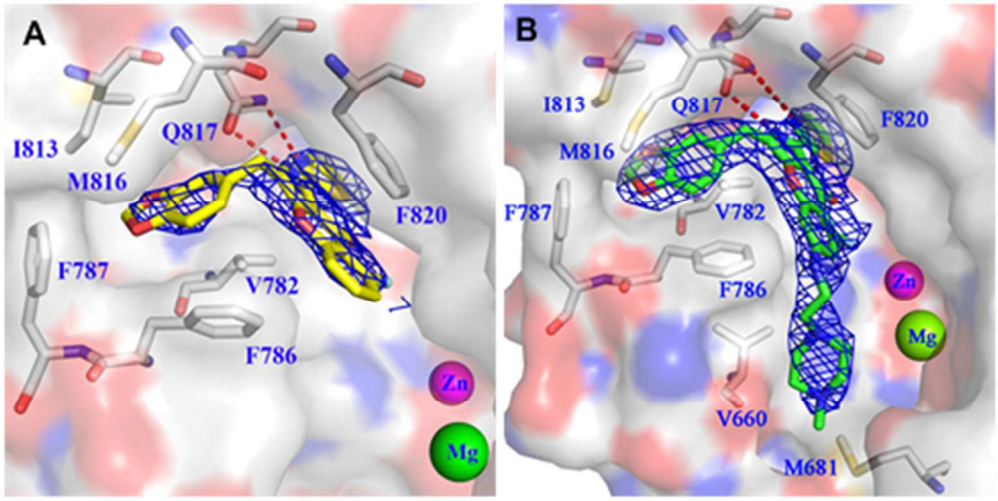

Figure 2. Co-crystal structure of the PDE5-11b and PDE5-17c complexes (PDB ID: 5ZZ2 and 6ACB). (A) Surface model for 11b (yellow sticks) binding. The dotted lines represent hydrogen bonds. (B) Surface model for 17c (green sticks) binding. The dotted lines represent hydrogen bonds.

221x110mm (200 x 200 DPI)

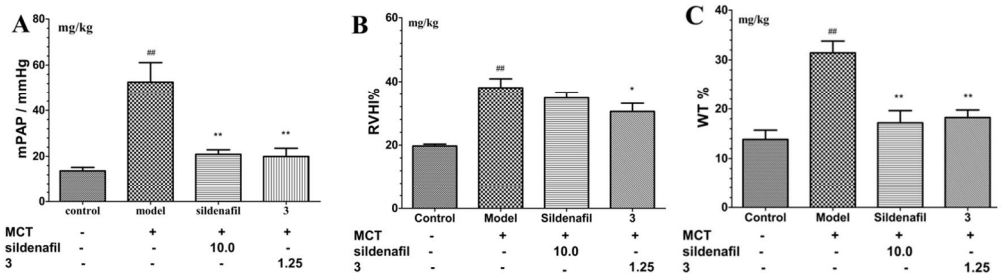

Figure 3. Pharmacodynamic effect of compound 3 on rats with PAH. (A) Reduction of pulmonary artery pressure by 3 and sildenafil citrate, which was induced by monocrotaline (MCT). The data is shown as the mean ± S.E.M (n = 6-9/group). Comparison of mPAP between groups: (##) $p < 0.01$ compared to the control group; (**) $p < 0.01$ compared to the model group. (B) Effects of 3 and sildenafil citrate on RVHI (Index of Right Ventricle Hypertrophy) of rats with PAH. Comparison of RVHI% between groups: (##) $p < 0.01$ compared to the control group; (*) $p < 0.05$ compared to the model group. (C) Effects of 3 and sildenafil citrate on the thickness of small pulmonary arteries of rats with PAH. Comparison of WT % between groups: (##) $p < 0.01$ compared to the control group; (**) $p < 0.01$ compared to the model group.

465x130mm (300 x 300 DPI)

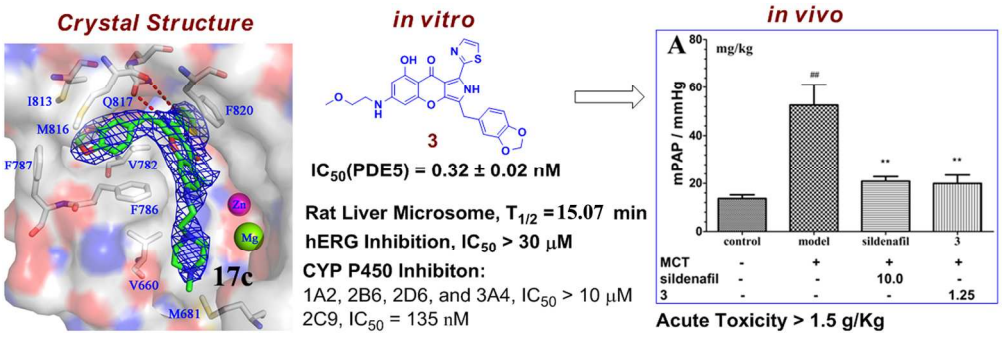

Table of Contents Graphic

303x99mm (200 x 200 DPI)